Investigation of Nitrogen Molecular Dynamics and Reaction Kinetics in an Industrial Ozone Generator

PI: Daniel E. Guerrero

Research Collaborators: Dr. Alfred Freilich, Dr. Stephen Kelty & Dr. Jose L. Lopez

Department of Chemistry and Biochemistry

SETON HALL UNIVERSITY
1856

Outline

- Introduction to Ozone Generation
- The Role of Nitrogen
- Preliminary Experiments
- Future Work
- Conclusion

What is Ozone?

- Tri-atomic form of oxygen.
- Most powerful commercial oxidizing agent available ($E^0 = +2.07V$).
- Unstable - must be generated and used onsite.
- Leaves a dissolved residual which ultimately converts back to oxygen.
- Relatively easy to manufacture.

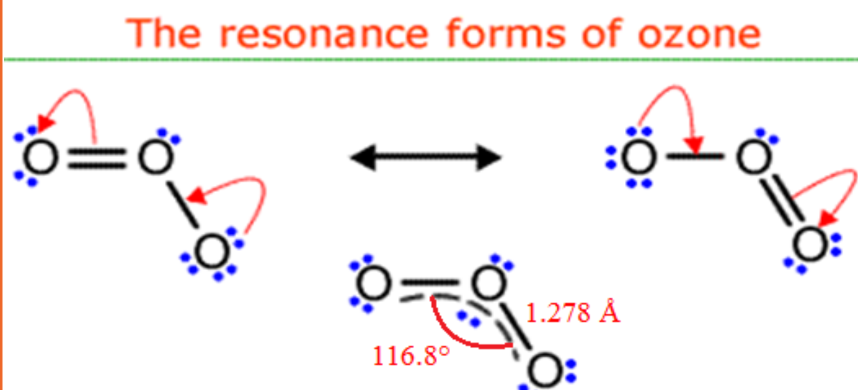

Figure 1. The 'averaged' structure of ozone showing the delocalized molecular orbital.

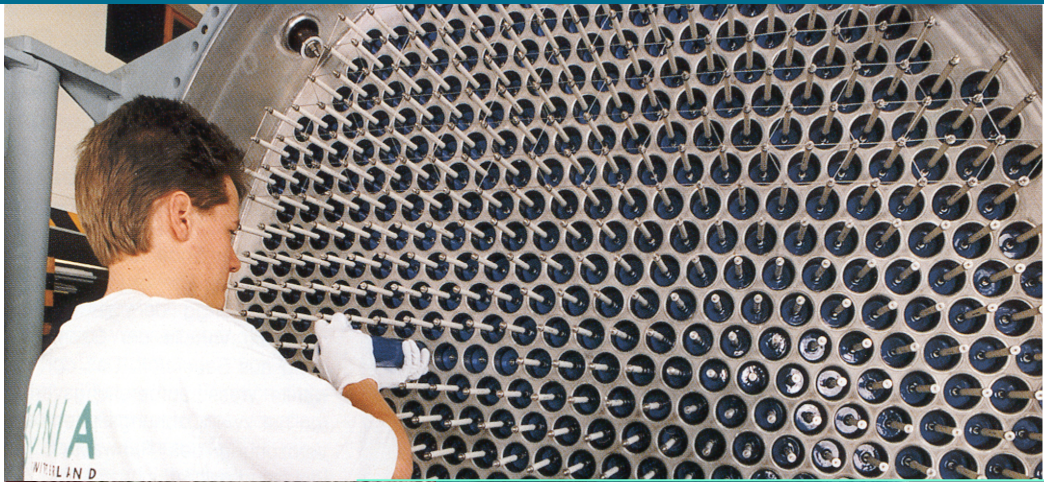

Figure 3. Ozone disinfection bubble diffusers.

Generation of Ozone

Dielectric Barrier Discharge (DBD)

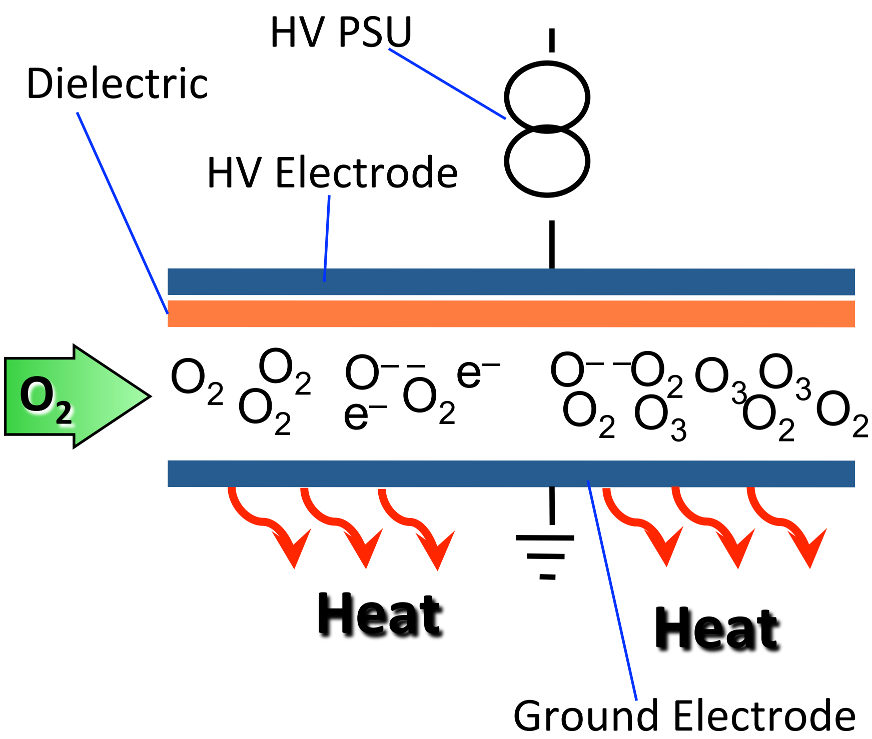

Figure 4. Ozone generator diagram.

$$3\,O_2 \rightleftharpoons 2\,O_3$$

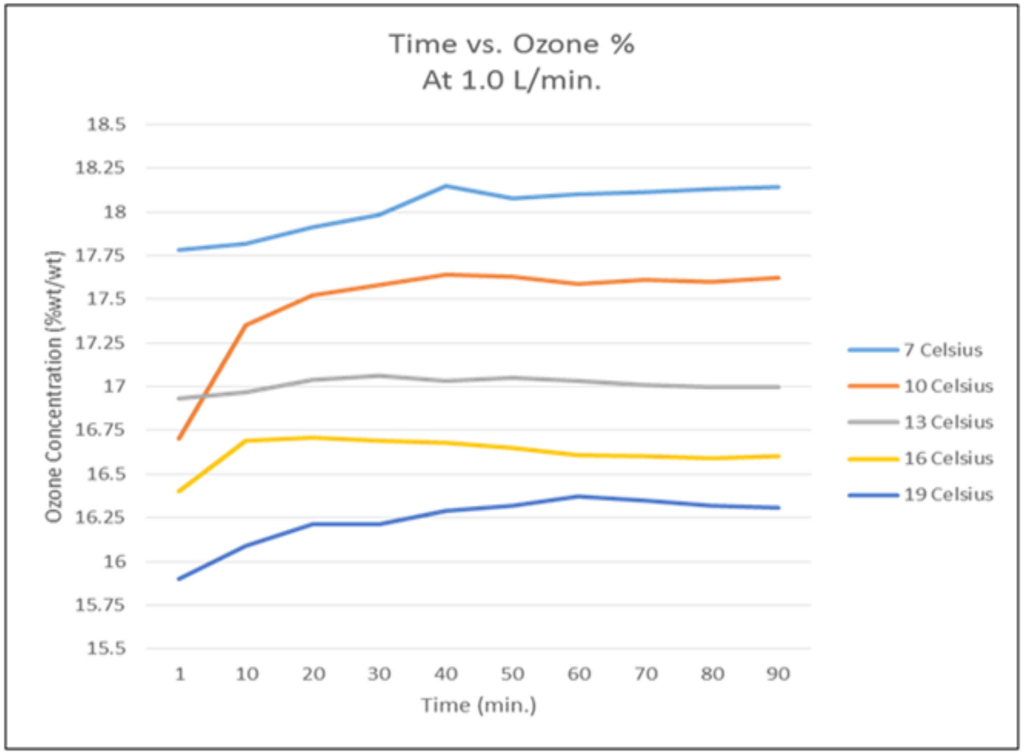

Figure 5. Water-cooled reactor with pure O_2 at 1.1 bar pressure and constant input power of 160 Watts.

SETON HALL UNIVERSITY 1856

Why Use Nitrogen?

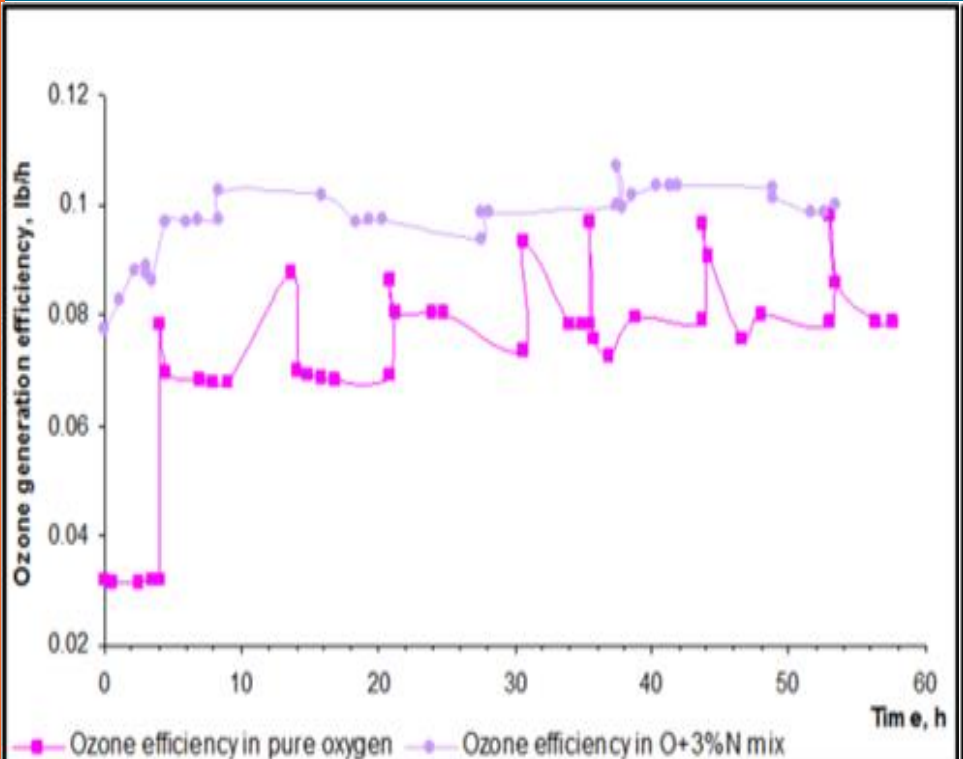

Figure 6. Plot of ozone production as a function of time with and without N_2.

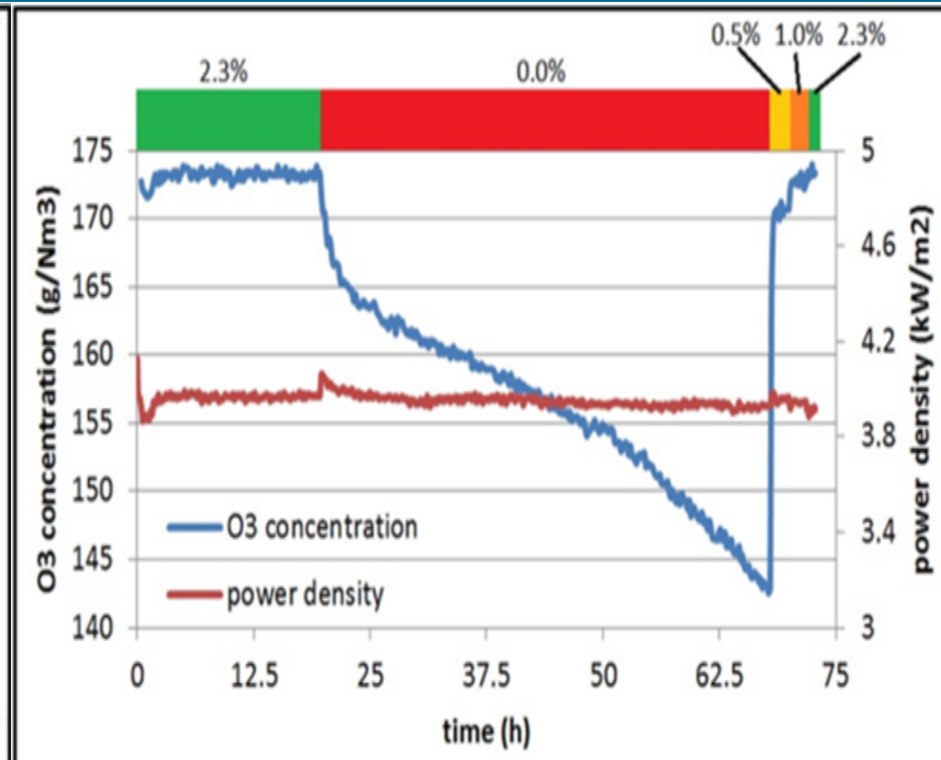

Figure 7. Plot of ozone production efficiency as a function of N_2 inclusion at constant power density and temperature

SETON HALL UNIVERSITY 1856

Plasma Temp. Study – Setup 1

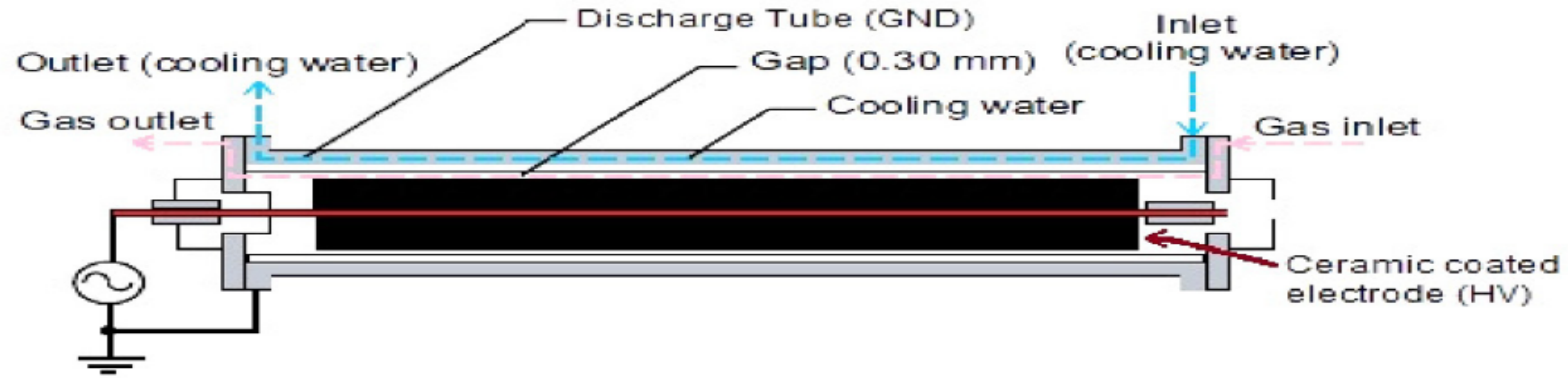

Fig. 4. Configuration of the ozone generator.

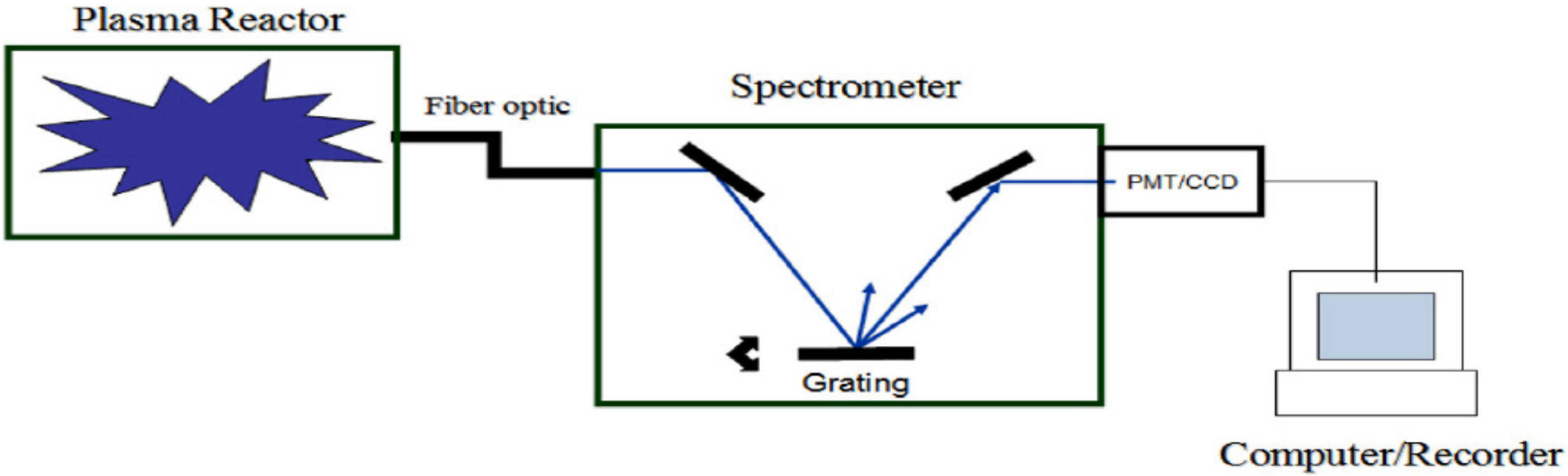

UV Emission Spectra – Setup 1

- Figure 3 shows relative emission intensities from a DBD ozone generator with a feed gas mixture of (O_2 + 3% N_2) at 2.2 bar pressure.

*

Species (system)	Transition
N_2 second positive	$C^3\Pi \rightarrow B^3\Pi$

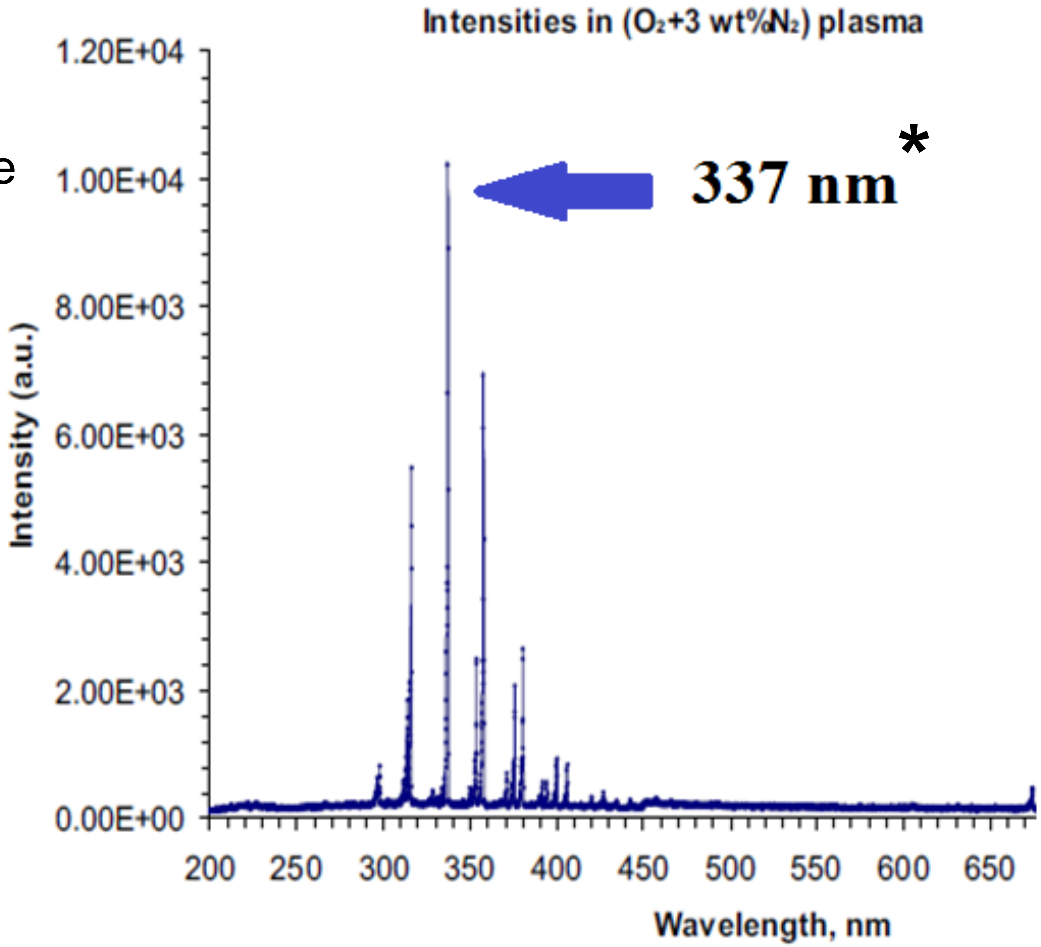

Preliminary Results – Setup 1

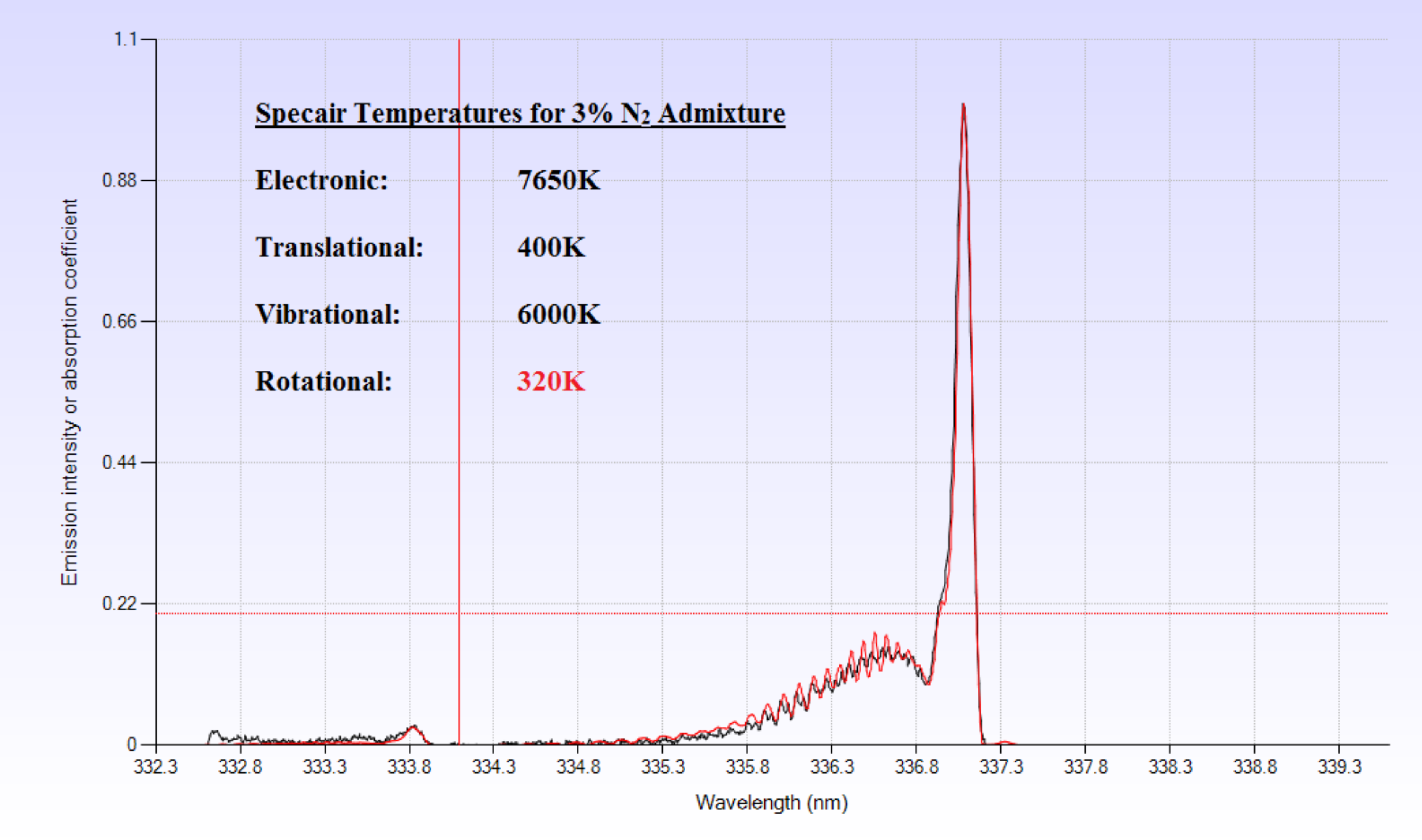

Preliminary Results – Setup 2

For measuring the temperature a type K thermocouple was glued with epoxy resin to the inner side of an LG-03 segment. The segment is a fairly massive metal body with a thin ceramic coating and no gas flow inside it. For this reason it is fair to assume that after a long enough operation time the temperature of the segment will be well homogenous and the measurement performed on the inner surface will be representative of the temperature on the ceramic surface.

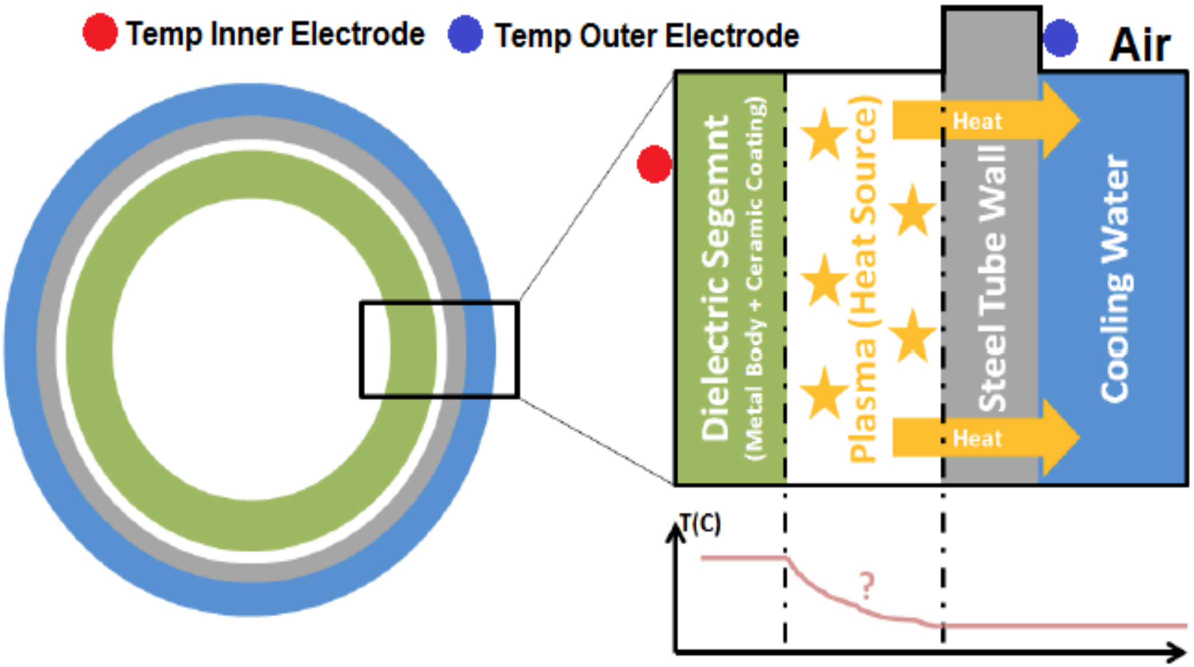

Recorded Temperature:

45.5 Degrees Celsius

~319 Kelvin

Figure 2: Detail of the experimental setup. The thermocouple is drawn along the piping and the homemade feedthrough.

Effect of N_2 Conc. on Gas Temp.

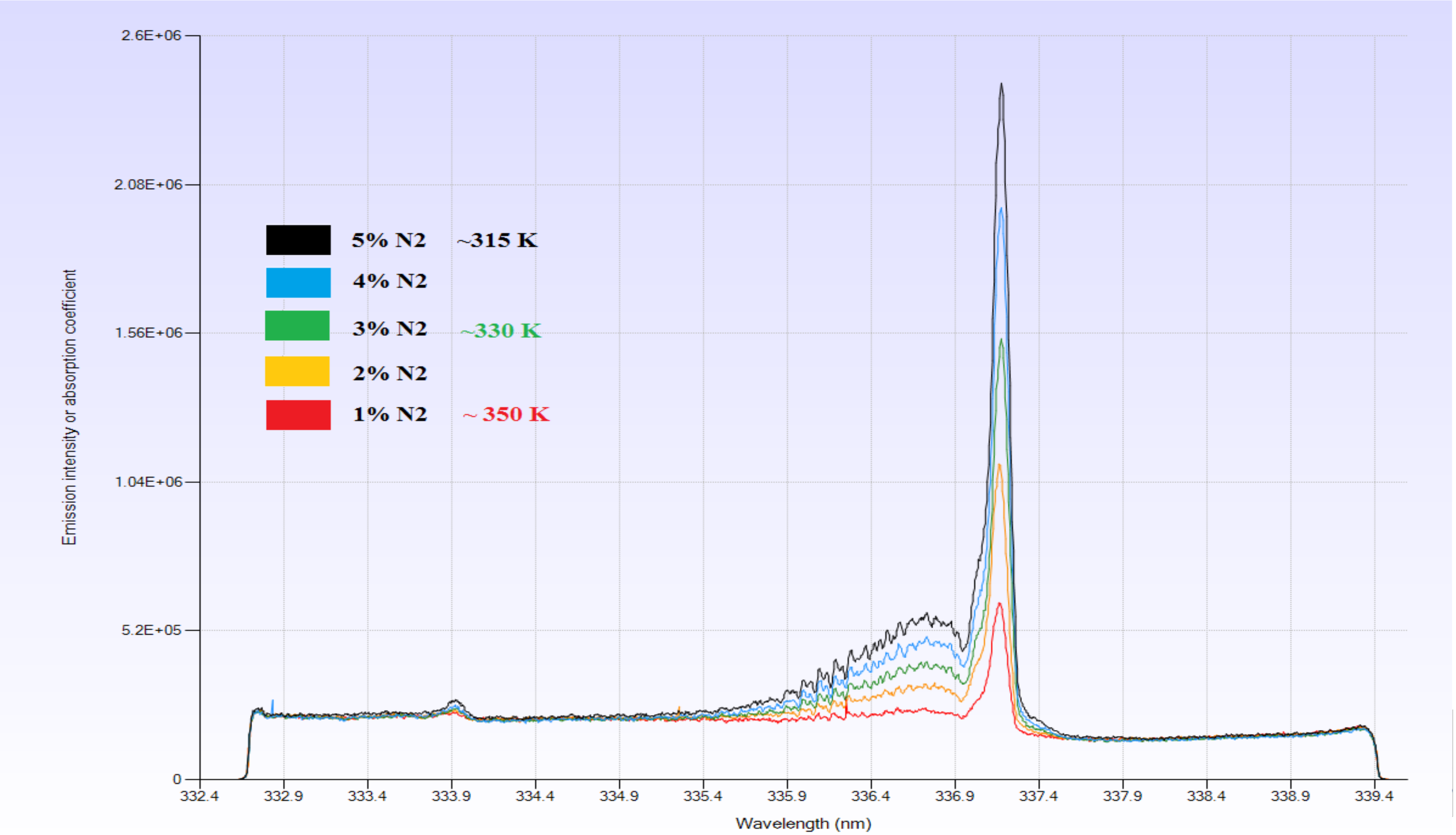

Effect of N_2 on Gas Temp. Cont.

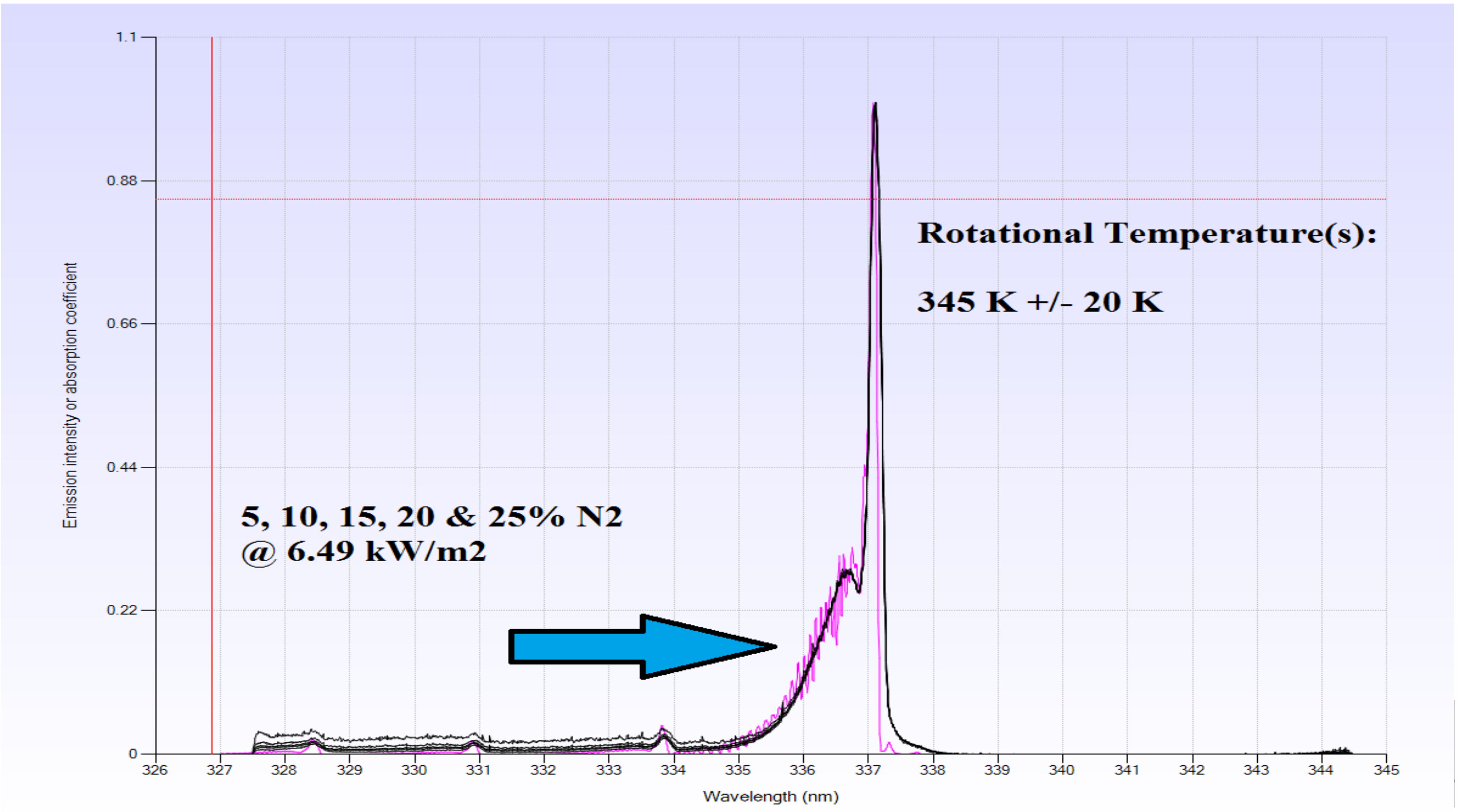

H_2O Temp and Pressure Effects

Target Values				Measured Values						
Trial #	Applied Power (kW/m^2)	Cooling Water Temp ©	Pressure (bars abs)	Applied Power (kW/m^2)	O3 (g/Nm^3)	Cooling Water Temp (deg C)	Outer Electrode Temp ©	Inner Electode Temp ©	Cooling Water Temp - Outer Electrode Temp ©	Gap Temp ©
1	2.0	3	2.2	2.12	113.4	5.7	7.3	14.5	1.6	8.8
4	2.0	5	2.2	2.23	113.1	17.2	19.1	28.3	1.9	11.1
7	2.0	3	2.2	2.19	112.7	30.3	30.0	42.0	-0.3	11.7
5	3.5	3	2.2	3.52	148.8	17.6	19.8	37.2	2.2	19.6
2	3.5	5	2.2	3.41	153.5	5.2	8.2	23.5	3.0	18.3
8	3.5	5	2.2	3.52	140.5	29.7	29.1	48.4	-0.6	18.7
3	5.0	3	2.2	4.96	180.0	5.3	10.6	33.3	5.3	**28.0**
6	5.0	5	2.2	5.01	171.5	17.3	20.7	45.5	3.4	**28.2**
9	5.0	30	2.2	4.96	159.5	29.9	31.0	56.4	1.1	**26.5**
10	3.0	17	2.2	3.11	155.0	17.3	20.7	34.5	3.4	15.5
11	5.0	17	2.2	4.97	149.0	17.2	21.0	44.5	3.8	**25.4**
12	3.0	17	2.2	3.12	96.2	17.1	20.1	34.8	3.0	16.2
13	5.0	17	2.2	4.98	89.7	17.5	20.9	43.8	3.4	24.6
14	3.0	17	1.6	2.99	155.4	17.6	19.6	34.4	2.0	15.8
15	5.0	17	1.6	4.75	148.2	16.9	20.9	44.6	4.0	25.7
16	3.0	17	2.8	3.21	162.7	17.4	20.1	35.6	2.7	16.9
17	5.0	17	2.8	5.15	150.4	17.6	21.5	46.6	3.9	27.1

H_2O Temp Effect

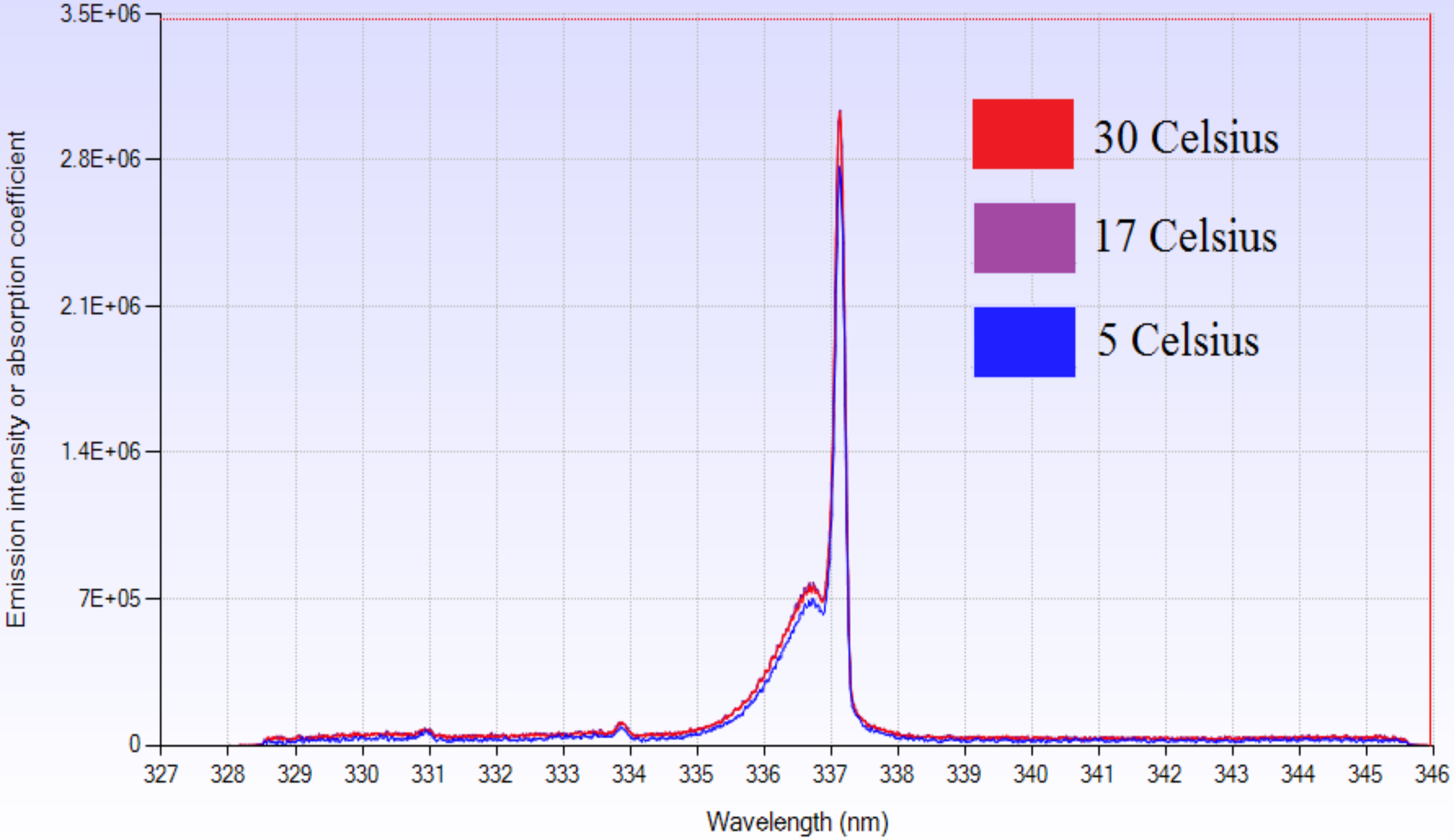

Working Hypothesis: Surface Effect

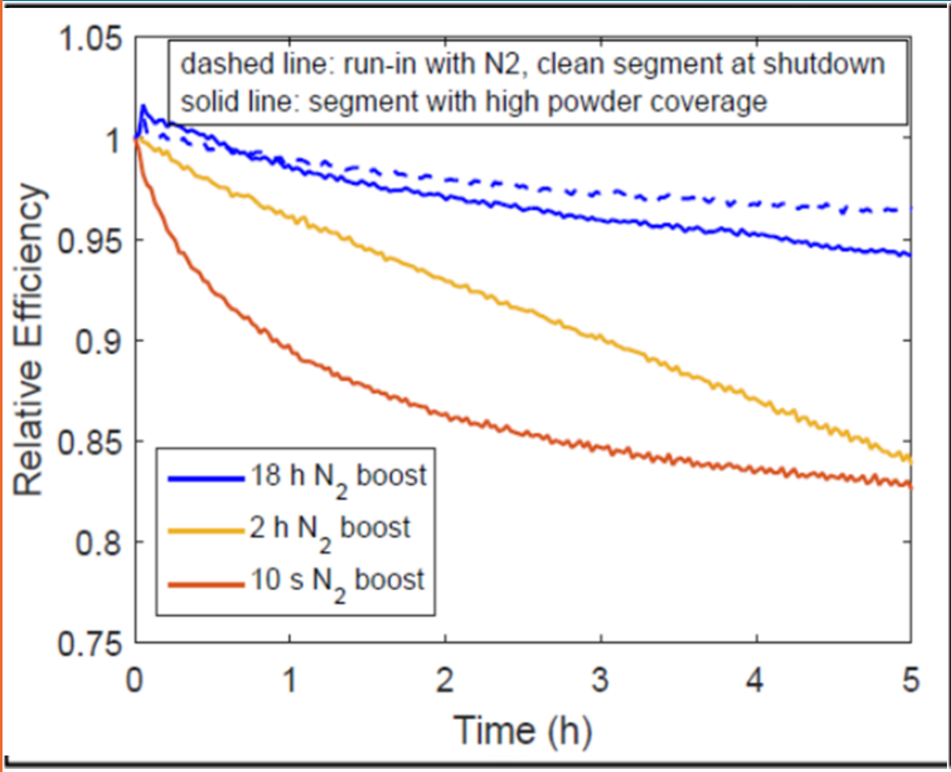

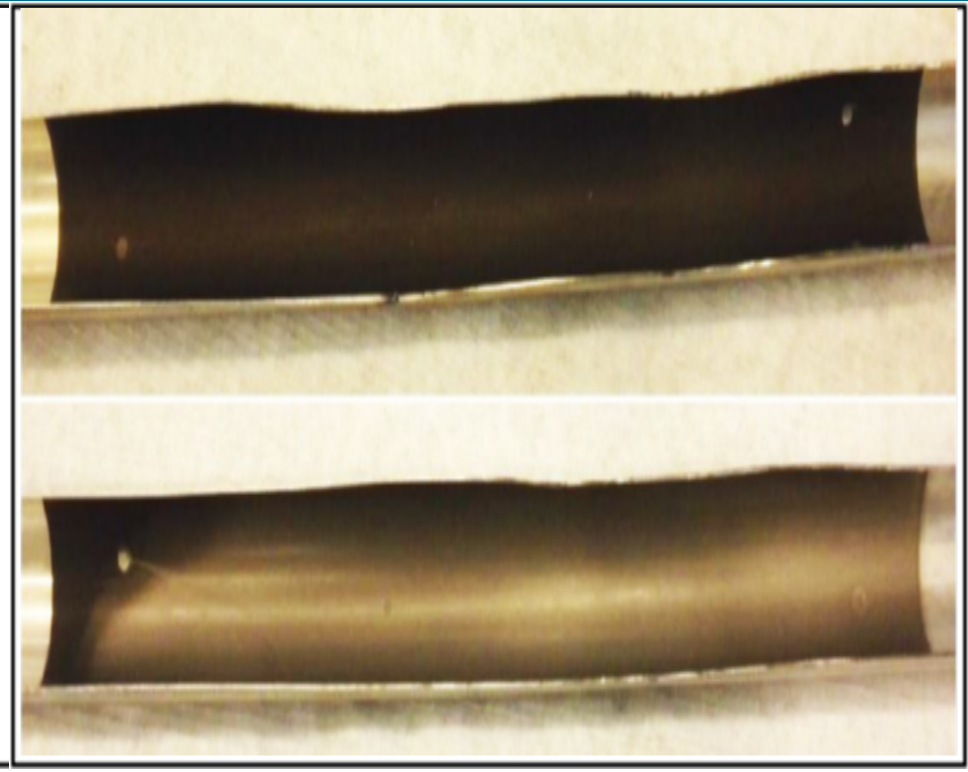

Figure 8. Time dependent evolution of ozone generation efficiency after shutdown of N_2 supply. During the experiments illustrated with solid lines, the high voltage electrode was already covered in a powder because of prior N_2-free operation. The dashed line corresponds to N_2 shutdown initiated with no prior N_2-free operation, i.e. a relatively powder-free electrode.

Figure 9. Photograph of the discharge tube when operated without N_2 (top) and with 2.3% N_2 (bottom).

SETON HALL UNIVERSITY 1856

Gas Effluent After N_2 Shutoff

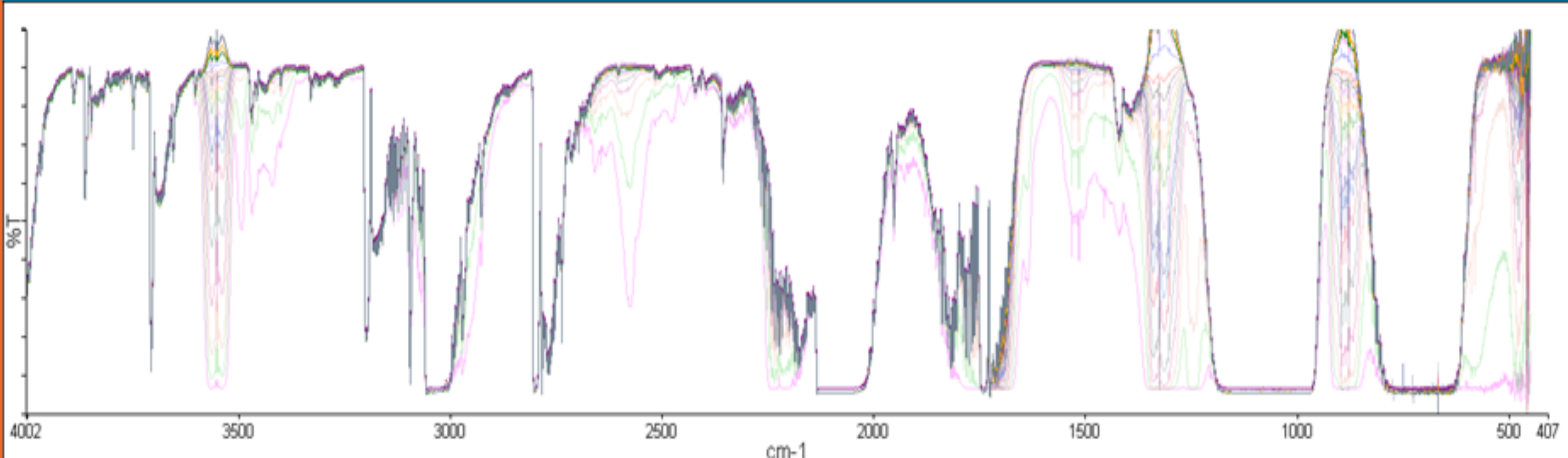

Name	Description
10 min pure O2 - 75% Pwr	Sample 017 By Researcher Date Friday, Nove...
10 min 10%N2 - 75% Pwr	Sample 018 By Researcher Date Friday, Nove...
2 min after n2 shutoff - 75...	Sample 019 By Researcher Date Friday, Nove...
5 min after shutoff	Sample 020 By Researcher Date Friday, Nove...
8 min after	Sample 021 By Researcher Date Friday, Nove...
11 min after n2 shutoff	Sample 022 By Researcher Date Friday, Nove...
15 min after n2 shutoff	Sample 023 By Researcher Date Friday, Nove...
20 min after N2 shutoff	Sample 024 By Researcher Date Friday, Nove...
25 min after n2 shutoff	Sample 025 By Researcher Date Friday, Nove...
30 min after n2 shutoff	Sample 026 By Researcher Date Friday, Nove...
35 min after N2 shutoff	Sample 027 By Researcher Date Friday, Nove...
40 min after n2 shutoff	Sample 028 By Researcher Date Friday, Nove...
45 min after N2 shutoff	Sample 029 By Researcher Date Friday, Nove...
50 min after N2 shutoff	Sample 030 By Researcher Date Friday, Nove...
60 min after n2 shutoff	Sample 031 By Researcher Date Friday, Nove...
75 min after n2 shutoff	Sample 032 By Researcher Date Friday, Nove...
90 min after n2 shutoff	Sample 033 By Researcher Date Friday, Nove...
105 min after n2 shutoff	Sample 034 By Researcher Date Friday, Nove...
120 min after N2 shutoff	Sample 035 By Researcher Date Friday, Nove...
155 min after N2 shutoff	Sample 036 By Researcher Date Friday, Nove...

Figure 10. FT-IR plot of reaction chamber effluent as a function of time following N_2 shutoff in the feed gas.

Gas Effluent After N_2 Shutoff

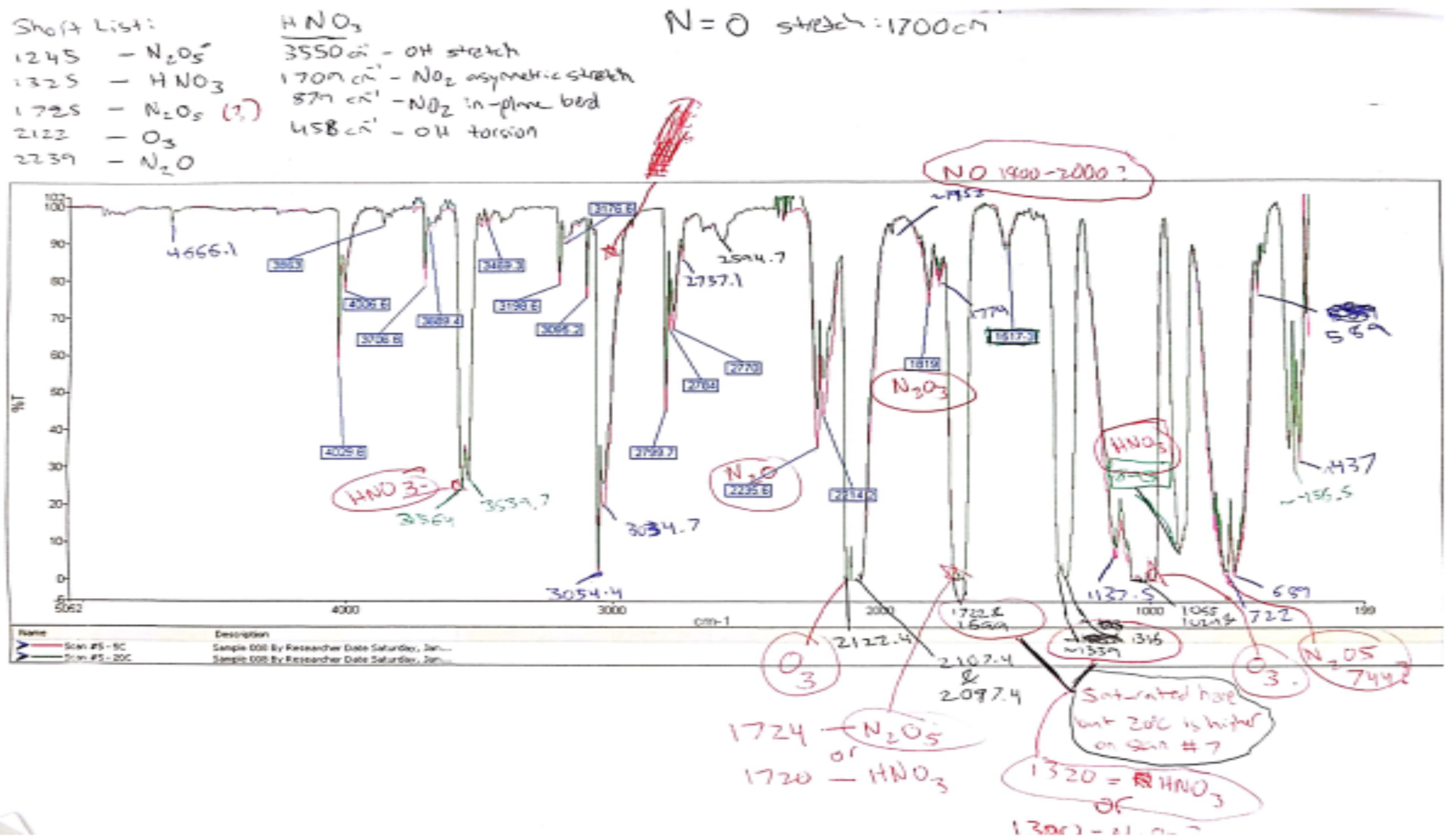

Gas Effluent After N_2 Shutoff

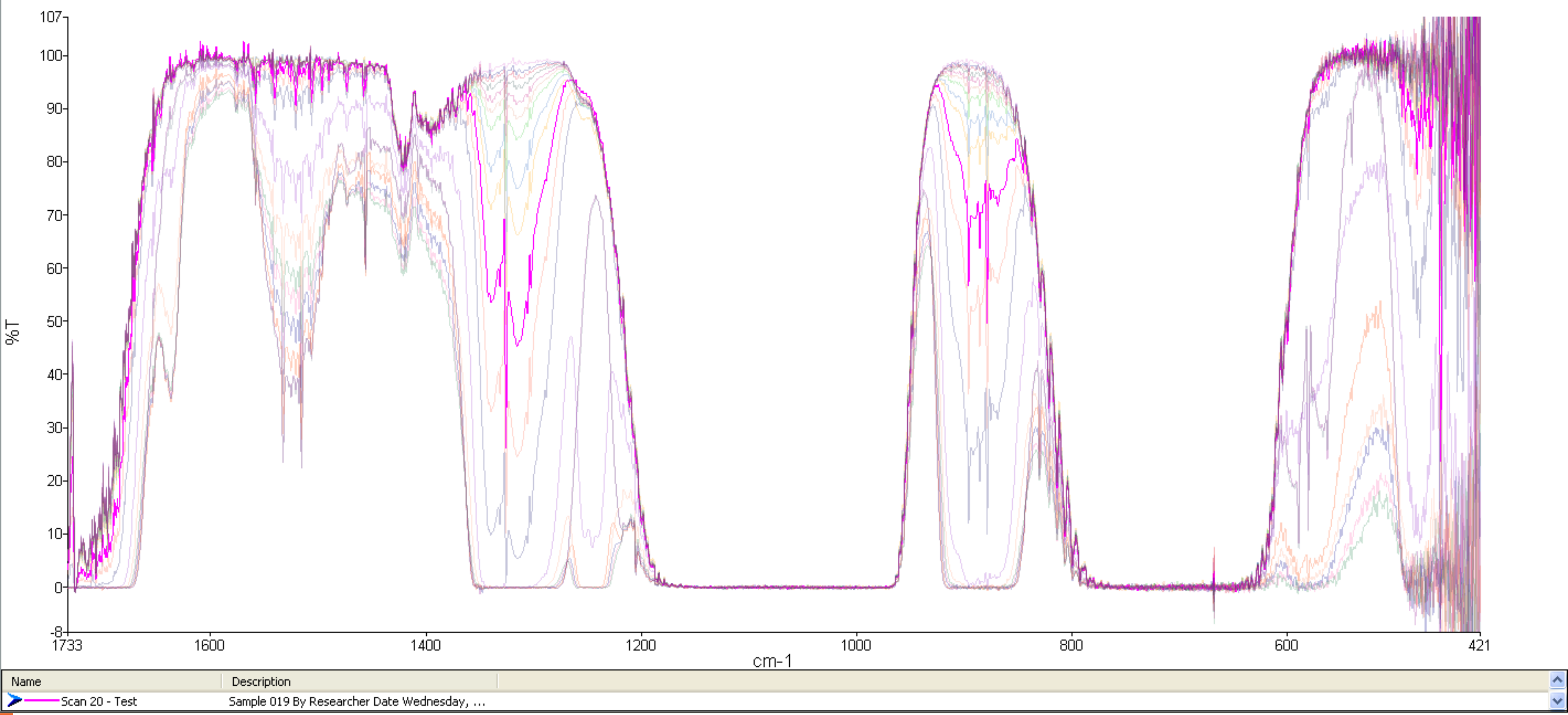

SETON HALL UNIVERSITY 1856

Proposed Study

1. Calculate the absorption thermodynamics (adsorption equilibria) on steel surfaces (Cr_2O_3, Fe_2O_3) by NOx adsorbates (N_2O, N_2, NO, NO_2, N_2O_5, NO_4).

2. Model the above results as Langmuir isotherms of physisorbed adsorbates.

3. Determine the temperature dependence of surface coverage from the equilibrium constants.

4. Compare the calculated temperature dependencies (and dominate adsorped species) against experimental evidence.

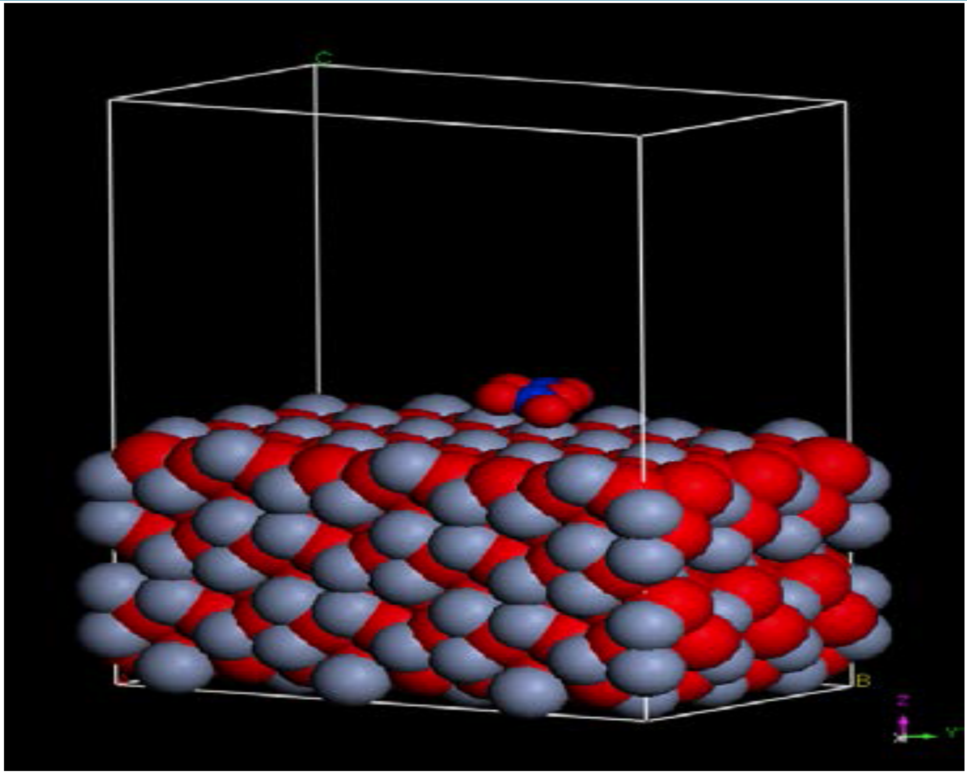

Figure 11. Input schematic of N_2O_5 on Cr_2O_3 surface.

SETON HALL UNIVERSITY 1856

Summary

- Nitrogen concentration appears to have a significant impact on gas temperature.
- However, the methodology by which the effects of N_2 concentration dictates gas temperature is not clear.
- Ozone production (output) also appears to be related to a surface effect on the electrode surfaces.
- A deeper investigation into the 3rd-body collisional process and surface chemistry is needed.

References

1. Koppenol, W. H., Reactions Involving Singlet Oxygen and the Superoxide Anion Nature 1976, 262, 420 421.
2. Pietscha, G. J.; Gibalov, V. I., Dielectric Barrier Discharges and Ozone Synthesis Pure & Appl. Chem. 1998, 70, 1169-1174.
3. Murai, A.; Yamabe, C.; Ihara, S., A Study of Ozone Formation on the Surfaces of Electrodes Ozone: Sci Eng. 2010, 32, 153-160.
4. Lee, H. M.; Chang, M. B.; Wei, T. C., Kinetic Modeling of Ozone Generation Via Dielectric Barrier Discharges Ozone: Sci Eng. 2004, 26, 551-562.
5. Batakliev, T.; Georgiev, V.; Anachkov, M.; Rakovsky, S.; Zaikov, G. E., Ozone Decomposition Interdisp. Toxicol. 2014, 7, 47-59.
6. Vosko, S. H.; Wilk, L.; Nusair, M., Accurate Spin-Dependent Electron Liquid Correlation Energies for Local Spin Density Calculations: A Critical Analysis Can. J. Phys. 1980, 58 1200-1211.
7. Kresse, G.; Hafner, J., Ab Initio Molecular Dynamics for Liquid Metals Phys. Rev. B 1993, 47, 588.
8. Kresse, G.; Hafner, J., Ab Initio Molecular-Dynamics Simulation of the Liquid-Metal–Amorphous-Semiconductor Transition in Germanium Phys. Rev. B 1994, 49, 14251.
9. Kresse, G.; Furthmuller, J., Efficiency of Ab-Initio Total Energy Calculations for Metals and Semiconductors Using a Plane-Wave Basis Set Comput. Mat. Sci. 1996, 6, 15-50.
10. Kresse, G.; Furthmuller, J., Efficient Iterative Schemes for Ab Initio Total-Energy Calculations Using a Plane-Wave Basis Set Phys. Rev. B 1996, 54, 11169

SETON HALL UNIVERSITY 1856

Acknowledgements

Funding Partners:

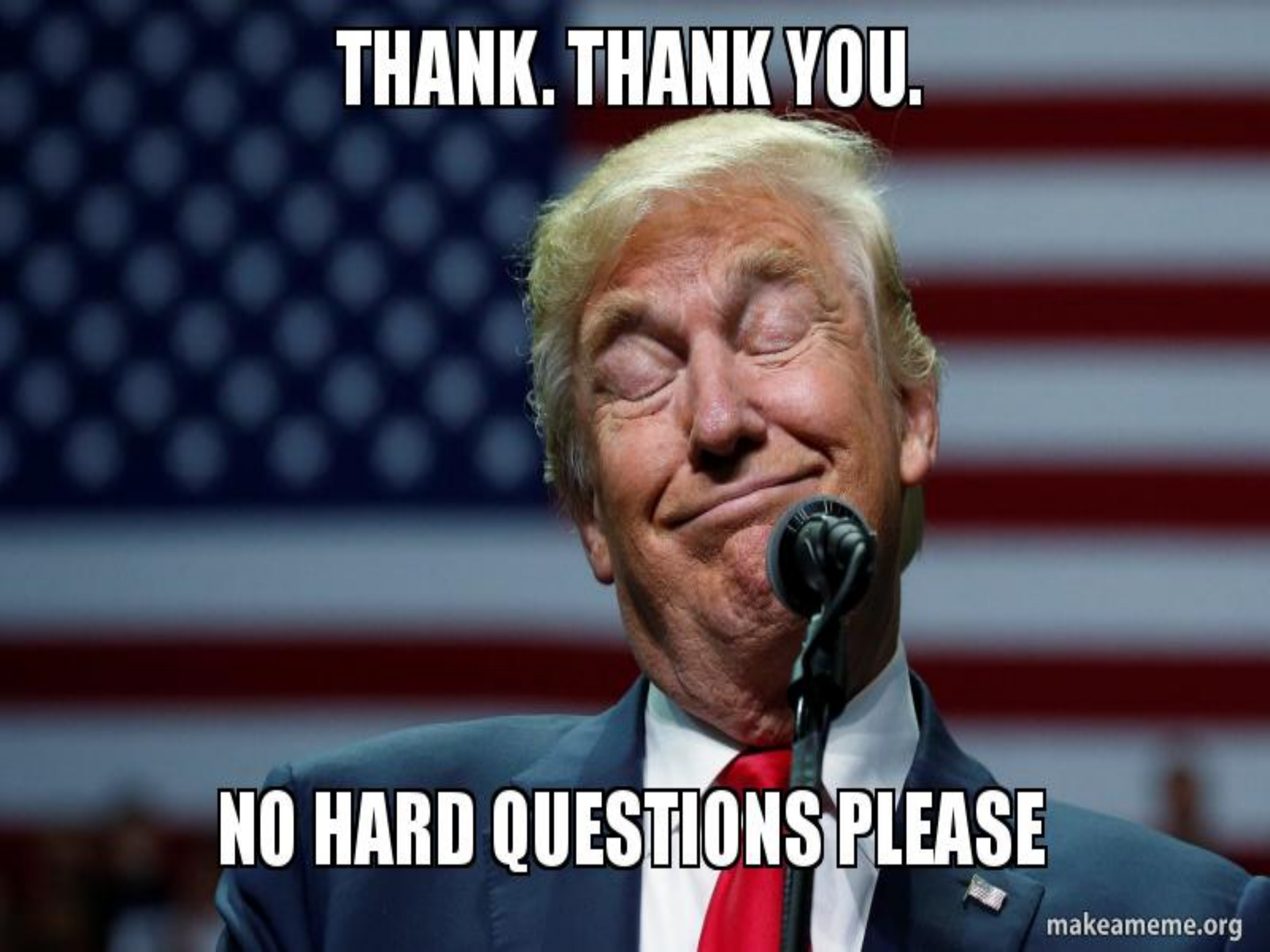
THANK. THANK YOU.
NO HARD QUESTIONS PLEASE
makeameme.org

Appendix

1. Plasma temperature study – UV emission spectroscopy, Specair analysis, thermocouple tests, & cooling water variation testing. [**Slides 10 – 18**]
2. Collisional and radiative processes within a plasma. [Slides 19 – 22]

SETON HALL UNIVERSITY 1856

Collisional and Radiative Processes

- The processes that determine the properties of non-thermal plasmas are collisions involving the plasma electrons and other plasma constituents.

- The charge carrier production is governed by
  - Direct ionization of ground state atoms and/or molecules
  - Step-ionization of an atom/molecule that is already in an excited and, in particular, a long-lived metastable state

- The generation of chemically reactive free radicals by electron impact dissociation in molecular plasmas is an important precursor for plasma chemical reactions.

SETON HALL UNIVERSITY 1856

Electron-Atom Collisions

$e + A \rightarrow A^{*/m} + e'$ $A^* \rightarrow A + h\nu$	Excitation of atoms Spontaneous de-excitation
$e + A^{*/m} \rightarrow A + h\nu + e'$	Collision-induced de-excitation
$e + A \rightarrow A^+ + e'$	Ionization of atoms
$e + A^{*/m} \rightarrow A + e' + E_{kin}$	Super-elastic collisions
$e + A^m \rightarrow A^* + e'$	Step-wise excitation
$e + A^m \rightarrow A^+ + e'$	Step-wise ionization

K. Becker and A. Belkind. ‘Introduction to Plasmas’. *Vacuum Technology & Coating (September 2003)*

SETON HALL UNIVERSITY 1856

Electron-Molecule Collisions

e + AB → AB$^{*/m}$ + e’ AB* → AB + *hv*	Excitation of molecules Spontaneous de-excitation
e + AB$^{*/m}$ → AB + *hv* + e’	Collision-induced de-excitation
e + AB → A$^{*/m}$ + B + e’	Dissociation of molecules
e + AB → AB^{+} + e’	Ionization of molecules
e + AB → A^{+} + B + e’	Dissociative ionization of molecules
e + AB → A^{+} + B + e’	Dissociative attachment of molecules
e + A^{+} → A + *hv*	Radiative recombination of an atomic ion
e + A^{+} + e’ → A + *e’*	3-body dielectronic recombination
e + A^{+} + M → A + M + *e’*	3-body heavy particle recombination
e + AB^{-} → A + B	Dissociative attachment of molecular negative ions

K. Becker and A. Belkind. ‘Introduction to Plasmas’. *Vacuum Technology & Coating (September 2003)*

Heavy Particle Collisions

$A + B^+ \rightarrow A^+ + B$	Charge transfer
$A + B^m \rightarrow A^+ + B + e$	Penning ionization
$A^m + A^m \rightarrow A^+ + A + e$	Pair ionization
$A^* + A \rightarrow A_2^+ + e$	Hornbeck-Molnar ionization
$A^+ + BC \rightarrow AC^+ + B$	Ion-molecules reaction
$A^{*/m} + BC \rightarrow AC + B$	Chemical reaction
$R + BC \rightarrow RC + B$	Chemical reaction with plasma radical, R

K. Becker and A. Belkind. 'Introduction to Plasmas'. *Vacuum Technology & Coating (September 2003)*

SETON HALL UNIVERSITY 1856